Dalton Transactions

ROYAL SOCIETY OF CHEMISTRY

PAPER

View Article Online
View Journal | View Issue

Cite this: *Dalton Trans.*, 2026, **55**, 4102

Uranium tetrafluoride *via* direct conversion of uranium dioxide using silver bifluoride in an ionic liquid medium

Parveen Kumar Verma, Frederic Poineau, Jason Victor and Kenneth Czerwinski *

Conventional methods to prepare crystalline uranium tetrafluoride (UF_4) involve the fluorination of uranium fluoride (UO_2) with corrosive chemicals (*i.e.*, $HF_{(g)}$) at elevated temperatures. Here, a novel method for producing UF_4 in a room temperature ionic liquid (RTIL) medium is presented. This method involves the fluorination of UO_2 in 1-methyl-1-butyl piperidinium bis(trifluoromethylsulfonyl)imide using silver bifluoride (SBF). The effect of RTIL volume, temperature, and water content on reaction yields and products is discussed. The volume of RTIL and reaction temperature are critical parameters in the formation of crystalline UF_4. The reaction of UO_2 with SBF at 200 °C with an RTIL volume of 0.5 mL gives crystalline UF_4 with the highest yield (94%). The presence of water in the RTIL led to the formation of hydrated UF_4, while the reaction performed at 150 °C resulted in amorphous UF_4.

Received 11th November 2025,
Accepted 10th February 2026

DOI: 10.1039/d5dt02703a

rsc.li/dalton

Introduction

Uranium tetrafluoride is a key material in the nuclear industry,[1–5] it occurs in the UF_6 enrichment/deconversion cycle,[4–8] it is used as a precursor for uranium metal production[9] and plays an important role in molten salt reactors.[10–13] Most of the reported methods for the preparation of UF_4 involve the use of hazardous corrosive fluorinating agents, *i.e.*, $HF_{(aq)}$ or $HF_{(g)}$,[14] and $F_{2(g)}$[5,6,15] at high temperatures (~550 °C). Research has explored alternative fluorination methods that involve mild fluorinating agents such as $NF_{3(g)}$[6,16–18] and bifluoride salts (AHF_2: A = NH_4, Ag).[3] Recent works have also used room temperature ionic liquids (RTIL) alone or in combination with HPF_6 for UF_4 synthesis.[19,20] The use of RTILs has attracted significant attention in actinide separation, electrochemical recovery, synthesis, and catalysis. Their appeal arises from distinctive physicochemical properties, including high thermal stability, low vapor pressure, wide electrochemical window, low hydrophobicity, non-flammability, and strong ability to dissolve a variety of metal complexes.[21–25] The fluorination of alkaline earth (Sr), transition (Fe, Co, Zn, and Ir), and lanthanide (La, Ce, Pr, Nd, Sm, Eu, Er, and Y) metal species using BF_4^- and PF_6^- containing RTIL has been documented.[26–28] For the actinides, UF_4 was successfully prepared from the fluorination of UO_2 or uranium oxalate in 1-butyl-3-methylimidazolium hexafluorophosphate (C_4mim-PF_6) in the temperature range 180–150 °C.[19,20] In both studies, PF_6^- acts as the fluorinating agent, and the possible degradation of the RTIL occurred during the reaction. While HPF_6 is a promising fluorinating agent,[19] it decomposes to HF and PF_5 upon drying. The commercially available HPF_6 is an aqueous solution (60–65%) consisting of ~21 wt% H_2O, 6% HF, and 8% of the phosphoric acids (*i.e.*, HPO_2F_2, H_2PO_3F, and H_3PO_4).[29]

To prepare anhydrous UF_4 while preventing the RTIL degradation, the fluorination of UO_2 in a stable RTIL using mild fluorination agents is proposed. One class of stable RTIL that could be employed is those containing the bistriflimide (TFSI) anion. Previous studies have shown that RTILs containing the TFSI anion are stable towards hydrolysis and do not decompose with water or acids.[22,30] Concerning fluorination, it has been shown that silver bifluoride ($AgHF_2$, SBF) can effectively fluorinate uranium oxides.[3,31] Silver bifluoride exhibits several advantages over ammonium bifluoride, such as decomposition temperature (160 °C *vs.* 240 °C) and absence of byproducts (*i.e.*, NH_4F, NH_3, and NO_x) that could interfere during the reaction.[32] The fluorination of UO_2 with SBF in air gives mixed UF_4 products (UF_4, $UF_4{\cdot}xH_2O$ (x = 1.5–2)), and a N_2 atmosphere is required for the formation of anhydrous UF_4.[3,31] The fluorination of UO_2 with SBF in RTIL would present several advantages. The RTIL, as a medium, would provide homogeneous HF concentration for fluorination; it can also help in the formation of different UF_4 morphologies by tuning the reaction conditions. The addition of RTIL to the UO_2 powder minimizes handling and prevents health hazards.

Department of Chemistry and Biochemistry, University of Nevada Las Vegas, 4505 S. Maryland Parkway, Las Vegas, Nevada 89154, USA.
E-mail: czerwin2@unlv.nevada.edu

Here, a novel method for the preparation of anhydrous UF_4 was developed. This method involved the fluorination of UO_2 with SBF in 1-methyl-1-butyl piperidinium bis(trifluoromethylsulfonyl)imide (MBPi-TFSI). The effect of reaction parameters (RTIL volume, temperature, water content) on reaction yield and reaction products was investigated. The synthesis conditions enable control over the reaction pathway, allowing tuning of the UF_4 phase and hydration state through adjustment of reaction conditions.

Results and discussion

The experimental setup is similar to the one previously used to prepare uranium fluoride microstructures[3,31] and consists of an autoclave and a box furnace. Before performing the fluorination experiment with uranium, the stability of the RTIL in the absence and presence of SBF was evaluated (*vide infra*). In a typical fluorination experiment, uranium dioxide was suspended in the RTIL, and the fluorinating agent (SBF) was introduced in the autoclave but outside of the RTIL, and heated at the desired temperature for 24 hours. A scheme of the setup is shown in Fig. 1, and the detailed procedure is presented in the Experimental section. Following fluorination, the uranium products were collected, washed, and analysed by powder X-ray diffraction (PXRD).

Evaluation of the RTIL for UF_4 synthesis

To evaluate MBPi-TFSI as the medium for the reaction, its stability was studied by TGA and FTIR spectroscopy in the presence and absence of SBF as a function of temperature. The relevant conditions are listed in Table 1.

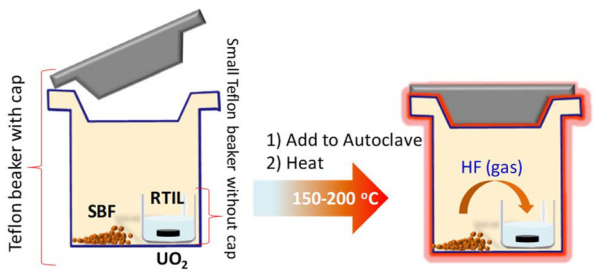

Fig. 1 Experimental setup used for the fluorination of UO_2 in RTIL.

Table 1 The experimental conditions (*T* and SBF mass) used to evaluate the stability of the RTIL and the observation/product after 24 hours of reaction with 2 mL of RTIL

T (°C)	SBF (mg)	Observation
200	0	Color change[a]
150	0	No color change
200	312.0 mg (inside RTIL)	Ag metal
200	318.6 mg (outside RTIL)	Color change[a]

[a] Color change from clear to brown.

Previous TGA studies showed TFSI-based RTILs to be stable up to 350 °C.[32,33] Initial experiments (Fig. S1, SI) have shown that the thermal treatment of SBF in RTIL produces Ag metal (Fig. S2 and S3). Silver metal will likely be congruently recovered with the uranium product, affecting both product yield and purity. Control experiment with *in situ* SBF in the absence of UO_2 powder also resulted in Ag metal, suggesting no involvement of UO_2 in Ag metal formation (Fig. S4). Consequently, the fluorination of UO_2 will be performed *ex situ*, with SBF outside the RTIL (see Fig. 1).

Previous TGA studies have shown the RTIL to be thermally stable.[32,33] Here, a noticeable color change from clear to brown was observed after treatment of MBPI-TFSI at 200 °C (Fig. S5). Similar color changes were reported for C_4mimPF_6 at 180 °C[20] and for butyl-methylpyrrolidinium-TFSI and butyl methyl-imidazolium-TFSI at <250 °C.[34] Here, the color changes suggest possible thermal degradation or chemical modification of the RTIL under the ionothermal conditions. Typically, TGA studies show the temperature of degradation of the bulk RTIL, whereas the color change may have started before bulk degradation.[34] The FTIR of the colored MBPI-TFSI does not show any difference with neat MBPI-TFSI (Fig. S6), suggesting the extent of degradation to be minor, but leads to the formation of chromophoric impurities.[35] Ionothermal studies indicate no color change at 150 °C (Fig. S7).

Fluorination of UO_2 in RTIL

The initial study shows MBPi-TFSI to be stable in the temperature range 150–200 °C. Based on initial results, the effect of SBF, RTIL volume, water content, and temperature of the reaction products and yields is examined. The experimental conditions and reaction products are presented in Table 2. An excess of SBF with respect to UO_2 (molar ratio SBF: UO_2 > 15) was used in all the reactions.

The role of the SBF as a fluorinating agent was confirmed by reacting UO_2 in MBPi-TFSI without SBF. The product obtained from the control reaction matches well with the starting UO_2 powder (Fig. S3).[36] This eliminates the possibility of the TFSI anion as the fluorinating agent.

Effect of RTIL volume

At constant temperature, U/SBF ratio, and water content, a decrease of the RTIL volume should lead to an increase of HF concentration in the RTIL and consequently an increase of the fluorination rate. In this context, several reactions were performed at constant temperature, U/SBF ratio, and various volumes of RTIL (2, 1, and 0.5 mL). For reaction 1 (2 mL of MBPi-TFSI), a powder (Fig. S8) with a green color characteristic of UF_4 and a very weak diffraction pattern was obtained (Fig. 2). The green powder was further analysed by FTIR and TGA. The TGA shows a major mass loss near the melting point of UF_4 (1036 °C) (Fig. S9).[4] A small mass loss near 400 °C may be due to the presence of residual MBPi-TFSI in the solid after the isopropyl alcohol (IPA) washing. The FTIR spectrum of the product was recorded after several IPA washings.

Table 2 The experimental condition (*T*, UO_2 mass, SBF mass, RTIL volume) and the major product obtained after 24 hours of reaction

Reaction	*T* (°C)	RTIL (mL)	UO_2 (mg)	Pre-conditioning	SBF (mg)	Major U product (mg) (% yield)
1	200	2	39.6	No	374.0	UF_4 amorphous (42.1) (91.4%)
2	200	2	35.1	Yes	321.5	UF_4 amorphous (35.6) (87.3%)
3	200	1	39.9	No	370.2	UF_4 crystalline (40.1) (87.1%)
4	200	1	37.0	Yes	421.0	UF_4 crystalline (36.1) (83.9%)
5	200	0.5	39.5	No	374.1	UF_4 crystalline (43.5) (94.8%)
6[a]	200	0.5	38.8	No	384.5	UF_4 amorphous (39.4) (87.4%)
7	150	0.5	33.8	No	357.1	UF_4 amorphous (35.4)(90.1%)

Pre-conditioning: treated under vacuum for 24 hours at 50 °C. [a] RTIL saturated with water prior the reaction.

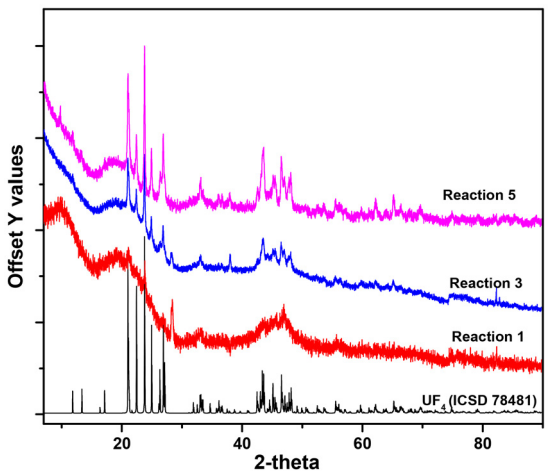

Fig. 2 PXRD of the product obtained from reactions 1, 3, and 5 and PXRD of UF_4 from the ICSD database (ICSD 78481).[37]

The decrease in the peak intensity >1000 cm^{-1} in the FTIR spectrum after the IPA washings suggested the presence of residual MBPi-TFSI in the solid used for the TGA studies (Fig. S10). Those results are consistent with the formation of amorphous UF_4.

Reaction 3 (1 mL) also resulted in a green solid but with higher crystallinity than reaction 1 (Fig. 2). The TGA of the solid recovered after reaction 3 shows only ~4% mass loss up to 600 °C, likely due to water, residual IPA, or RTIL (Fig. S11).

The primary source of water in the reaction is due to the conversion of UO_2 to UF_4 (eqn (1)).

$$UO_{2(S)} + 4HF_{(g)} \rightarrow UF_{4(s)} + 2H_2O_{(g)} \quad (1)$$

Though the reaction is performed at 200 °C, a small amount of water may be present in MBPi-TFSI, resulting in the water coordination to the precipitated UF_4. The PXRD of the recovered sample of reaction 3 after TGA shows the predominant presence of crystalline UF_4 (Fig. S12).

Reaction 5 (0.5 mL) led to an increase in UF_4 crystallinity (Fig. 2), with 94.8% yield. The TGA of the reaction 5 product shows <2.5% mass loss up to 600 °C, with prominent transitions at 45 °C, 175 °C, and 415 °C (Fig. S13). This transition may be arising from residual IPA/H_2O (45 °C and 175 °C) and RTIL (415 °C) in the anhydrous UF_4 product. The FTIR of the reaction 5 product was also recorded. Small but distinct peaks (Fig. S13) suggest the presence of residual IPA/H_2O and RTIL and corroborate well with the TGA data.

To better understand the effect of RTIL volume on reaction products, the concentration of HF in the RTIL (2 mL, 1 mL, and 0.5 mL) after reaction was determined. The HF concentration increases almost 2-fold with the reduction of RTIL volume from 2 mL (0.45 (±0.022) M) to 1 mL (0.92 (±0.025) M) and remains close to 1 M for the 1 mL (0.92 (±0.025) M) and 0.5 mL samples (0.99 (±0.031) M) (Fig. S14). This suggests HF saturation in the RTIL (~1 M) with 1 mL or lower volumes. The increase in the concentration of HF at a lower volume may be the factor driving the formation of crystalline material.

Effect of water

The RTILs absorb water even at room temperature, and the amount of water depends mainly on the nature of the anion of the RTIL, relative humidity, and temperature.[38–42] To understand the effect of the water content on the reaction product, a pre-conditioning drying step was introduced. In this pre-conditioning step, UO_2, MBPi-TFSI, and SBF were vacuum dried at 50 °C for 24 hours.

This process was used to dehydrate RTIL[43] and to remove absorbed moisture from solid surfaces. The reaction 2 product is very similar to the reaction 1 product from PXRD and TGA studies (Fig. S15 and S16). This suggests removal of water does not add to any major changes in the UF_4 product at 2 mL volume. No significant change in the PXRD of the product with and without pre-conditioning was observed even for 1 mL RTIL volume (Fig. S17), and hence, the pre-conditioning step was omitted in the further studies.

To further understand the role of water, an additional reaction with water-saturated RTIL was examined (reaction 7). A reaction performed using 2 mL of water-saturated MBPI-TFSI ([H_2O] ~11 000 ppm) at 200 °C with 0.5 mL RTIL resulted largely in amorphous UF_4 product, but with some peaks in the PXRD, suggesting formation of hydrated UF_4 (Fig. 3). This implies that excess water drives the reaction to the formation of amorphous and hydrated UF_4.

Effect of temperature

The studies using a control blank of MBPi-TFSI indicate no color change at 150 °C (Table 1 and Fig. S6). The UF_4 synthesis

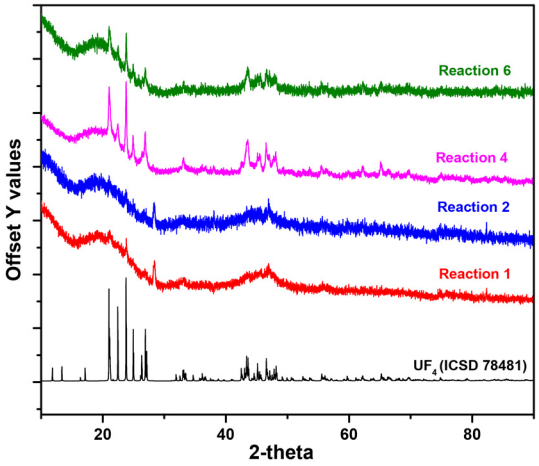

Fig. 3 PXRD of the product obtained from reactions 1, 2, 4, and 6 and PXRD of UF_4 from the ICSD database (ICSD 78481).[37]

at 150 °C with 0.5 mL of MBPi-TFSI results in an amorphous green product with PXRD peaks corresponding to UF_4. Under similar chemical conditions, reaction at 200 °C gives a more crystalline product, suggesting that a lowering in the temperature led to the formation of an amorphous product (Fig. 4).

The use of PXRD to analyse the solid crystalline material is well established, as is its ability to estimate or identify amorphous compounds as impurities. To confirm the product speciation, SEM-EDS studies were performed for reaction 5 (Fig. S18 and S19). It is important to mention that the elemental mapping by EDS suffers from poor detection of lower Z elements such as fluorine. The EDS mapping of the reaction 5 product gave an atomic ratio of 3.57 for F/U (Table S1), which is lower than the expected stoichiometric value due to analytical uncertainties associated with the quantification of fluorine and uranium. In combination with the PXRD results, these data support the assessment of the compound as UF_4. The SEM-EDS studies also indicate the absence of other secondary amorphous phases.

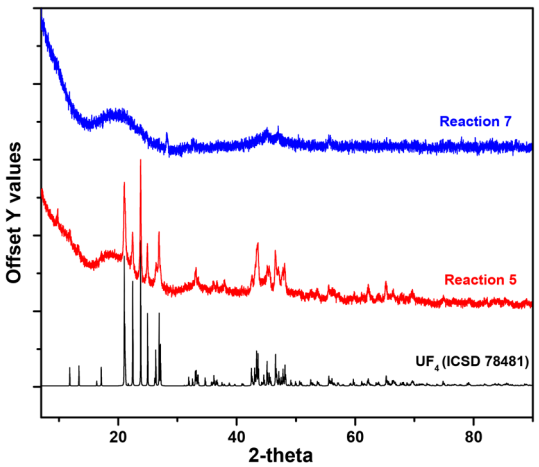

Fig. 4 PXRD of the product obtained from reactions 5 and 7 and PXRD of UF_4 from the ICSD database (ICSD 78481).[37]

Conclusions

In summary, a novel method for the preparation of anhydrous UF_4 in high yield has been developed. The method involves the fluorination of UO_2 in RTIL using SBF as a fluorinating agent. The volume of RTIL and temperature have an important role in the formation of crystalline UF_4. The reaction of UO_2 with SBF at 200 °C with an RTIL volume of 0.5 to 1 mL gives crystalline UF_4. The highest yield (94.8%) was obtained for a volume of 0.5 mL, though a color change in the MBPI-TFSI after the ionothermal reaction was observed, the FTIR spectra of the MBPI-TFSI after the reaction do not show any degradation. The presence of water in the MBPI-TFSI led to the formation of hydrated UF_4. The reaction at a lower temperature (150 °C) reduces thermal degradation (*i.e.*, color change) but primarily results in amorphous UF_4. The formation of crystalline UF_4 in MBPi-TFSI in high yield from the fluorination of UO_2 is promising, and this method could be transposed to other actinides. For example, PuF_4 could be prepared similarly using PuO_2 or Pu-oxalates as precursors. Current work is in progress, and results will be reported in due course.

Experimental

Materials and methods

Caution! ^{238}Uranium is an α emitter with E_{max} = 4.26 MeV. All the manipulations were performed in a designed radiochemistry laboratory equipped with fume hoods and HEPA filters.

Silver bifluoride (≥99%, Alfa Aesar), 1-methyl-1-propylpiperidinium bis(trifluoromethylsulfonyl)imide (iolitec, Germany), and UO_2 powder were used from the laboratory stock. The PXRD of the UO_2 powder confirms the phase purity (Fig. S20).

Fluorination of uranium dioxide in RTIL

For the uranium dioxide fluorination reactions, UO_2 powder and SBF were placed in autoclaves separated by a Teflon vial. Uranium dioxide (30–35 mg, 0.11–0.13 mmol) powder was mixed with different volumes of MBPI-TFSI (2 mL-0.5 mL), and placed in a 15 mL Teflon vial. The Teflon vial was then placed in the Teflon liner of an autoclave containing an excess of SBF (SBF: 300–350 mg; molar ratio [SBF]/[UO_2] > 15)(Fig. 1).

A pre-conditioning step was introduced in some samples to dry the reactants before the fluorination reaction. During the pre-conditioning step, the reactants UO_2, MBPi-TFSI, and SBF were vacuum dried at 50 °C for 24 hours.

All the fluorination reactions were conducted under air in a Parr model 4749 autoclave using a previously reported procedure.[44] The entire assembly was sealed and added to the autoclave, where it was heated for 24 hours using Thermo Scientific Thermolyne Benchtop Muffle Furnace (model FB1315M) at the predefined temperature.

Recovery of the solid UF_4

After fluorination, the green product was separated from MBPI-TFSI by centrifugation at 6000 RPM for 15 minutes. The MBPI-TFSI was transferred using a pipette, and the solid product was washed 2–3 times with isopropyl alcohol (IPA, 2 mL) to remove any residual MBPI-TFSI. The removed solid was dried at room temperature and used for further characterization. The FTIR spectrum of the dried solid product was recorded to ascertain complete removal of the MBPI-TFSI and IPA.

Solid product characterization

FTIR. The FTIR spectra were recorded using an Agilent 630 FTIR instrument. The solid was placed on the diamond crystal and pressed to avoid any air gap between the diamond crystal and the solid. One hundred scans were recorded and averaged for each FTIR measurement in the 650–4000 cm^{-1} range with 4 cm^{-1} resolution.

Powder X-ray diffraction studies. The powder X-ray diffraction (PXRD) measurements were performed on a XRDynamic 500 diffractometer (Anton Parr) with a fixed sample stage. The measurements were done with a Cu-K_α radiation source (λ = 1.54 Å) from 7° to 90° 2θ in Bragg–Brentano geometry. The PXRD patterns were analysed using the PC-PDF database or the ICSD database.

Scanning electron microscopy (SEM) measurements. The SEM–EDS analyses for the prepared sample were conducted with a Tescan Clara (Field-Emission scanning electron microscope). The elemental quantification was done with an Oxford EDS detector with an accelerating voltage of 15 kV at a working distance of 15 mm. The samples were mounted on carbon tape without coating.

TGA measurements. The TGA–DSC measurements were performed with a TA Instruments SDT 650 Discovery series TGA–DSC from 25–1300 °C with a heating rate of 20 °C per minute. All the samples were measured in alumina cups with lids under a constant flow of argon gas (100 mL min^{-1}) over the sample and balance.

Karl-Fisher titration. The water content in the MBPi-TFSI was measured using Karl Fisher titration. A known mass of the MBPI-TFSI was added to the anolyte and allowed to equilibrate for 10 seconds. The electrochemically generated I_2 was used for titration. The water saturation of the MBPI-TFSI was achieved by equilibrating an equal volume of the MBPI-TFSI with deionised water (resistivity 18.2 MΩ) for 1 hour. The MBPI-TFSI phase was separated by centrifugation at 6000 RPM for 5 minutes, and small aliquots of the MBPI-TFSI were used for the titration.

HF estimation. The HF concentration in the MBPi-TFSI phase was determined by both pH measurements and acid–base titration using phenolphthalein as an indicator. A known volume of the MBPI-TFSI (200–300 μL) was mixed with twice its volume of deionised water and vortexed. The two phases were separated by centrifugation at 5000 RPM for 10 minutes, and the acidity of the aqueous phase was determined. For pH measurement, the aqueous phase was diluted 60 times, and the pH of the resulting solution was recorded using thermofisher pH meter. For acid–base titration, an aliquot of 25–50 μL was added to deionised water and titrated with standard 0.1 M NaOH using phenolphthalein as an indicator.

Author contributions

Parveen Kumar Verma: conceptualization; data curation, formal analysis, investigation, methodology and writing – original draft. Frederic Poineau: conceptualization, supervision, writing – review and editing. Jason Victor: investigation and laboratory assistance. Kenneth Czerwinski: funding acquisition; conceptualization; supervision; writing – review and editing.

Conflicts of interest

There are no conflicts to declare.

Data availability

The data supporting this article have been included as part of the supplementary information (SI). Supplementary information is available. The supplementary information includes the experimental setup, photographs of the reaction products (RTIL color change and recovered solid product), XRD data of several reactions, TGA data, ATR-FTIR, and SEM-EDS. See DOI: https://doi.org/10.1039/d5dt02703a.

Acknowledgements

This research was performed using funding received from the DOE Office of Nuclear Energy's Nuclear Energy University Program under Consolidated Innovative Nuclear Research (CINR) Award No. DE-NE009302 titled SUSTAIN: Supporting Strategic Training of Adaptable and Integrated Nuclear Workforce. The authors would like to thank Mrs. Wendee Johns for program administration assistance and Mr. Quinn Summerfield for his expertise in laboratory operations. The authors are grateful to the UNLV Radiation Safety Office for their support.

References

1 K. R. Foster, J. Schorne-Pinto, R. E. Booth, A. Husek, M. Aziziha, H. B. Tisdale, B. W. N. Fitzpatrick, H. C. zur Loye, M. H. A. Piro and T. M. Besmann, *J. Fluor. Chem.*, 2025, **285–286**, 110449.
2 H. S. Booth, W. Krasny-Ergen and R. E. Heath, *J. Am. Chem. Soc.*, 1946, **68**, 1969–1970.
3 H. Jang and F. Poineau, *Mater. Adv.*, 2024, **5**, 8233–8237.

4 I. Grenthe, J. Drożdżyński, T. Fujino, E. C. Buck, T. E. Albrecht-Schmitt and S. F. Wolf, in *The Chemistry of the Actinide and Transactinide Elements*, Springer Netherlands, Dordrecht, 2008, pp. 253–698.
5 L. A. But, V. D. Vdovichenko, O. B. Gromov, A. N. Evdokimov, A. V. Ivanov, I. A. Logvinenko, P. I. Mikheev, D. V. Fedorova and V. V. Shilov, *Theor. Found. Chem. Eng.*, 2016, **50**, 884–889.
6 B. McNamara, R. Scheele, A. Kozelisky and M. Edwards, *J. Nucl. Mater.*, 2009, **394**, 166–173.
7 C. J. Higgins, K. I. Luebke, F. Poineau, K. R. Czerwinski and D. W. Hatchett, *J. Radioanal. Nucl. Chem.*, 2022, **331**, 5205–5213.
8 C. D. Scott, J. B. Adams and J. C. Bresee, *Ind. Eng. Chem. Process Des. Dev.*, 1964, **3**, 266–270.
9 D. S. Arnold, C. E. Polson and E. S. Noe, *JOM*, 1956, **8**, 637–639.
10 S. Rouquette-Sanchez, J. Finne and G. S. Picard, in *Proceedings - Electrochemical Society*, 2006, vol. PV 2004–24, pp. 738–748.
11 G. L. Fredrickson, G. Cao, R. Gakhar and T. S. Yoo, *Molten Salt Reactor Salt Processing – Technology Status*, Idaho Falls, ID (United States), 2018.
12 J. Uhlíř, *J. Nucl. Mater.*, 2007, **360**, 6–11.
13 M. W. Rosenthal, P. R. Kasten and R. B. Briggs, *Nucl. Appl. Technol.*, 1970, **8**, 107–117.
14 B. P. Aleksandrov, E. B. Gordon, A. V. Ivanov, A. A. Kotov and V. E. Smirnov, *J. Phys.: Conf. Ser.*, 2016, **751**, 012012.
15 P. Souček, O. Beneš, B. Claux, E. Capelli, M. Ougier, V. Tyrpekl, J. F. Vigier and R. J. M. Konings, *J. Fluor. Chem.*, 2017, **200**, 33–40.
16 R. D. Scheele, B. K. McNamara, A. M. Casella, A. E. Kozelisky and D. Neiner, *J. Fluor. Chem.*, 2013, **146**, 86–97.
17 R. Scheele, B. McNamara, A. M. Casella and A. Kozelisky, *J. Nucl. Mater.*, 2012, **424**, 224–236.
18 A. M. Casella, R. D. Scheele and B. K. McNamara, *AIP Adv.*, 2015, **5**, 127230.
19 E. Ciprian, B. J. Foley, T. L. Spano, A. Miskowiec, T. Shehee and A. E. Hixon, *J. Nucl. Mater.*, 2025, **615**, 155983.
20 F. Joly, P. Simon, X. Trivelli, M. Arab, B. Morel, P. L. Solari, J. F. Paul, P. Moisy and C. Volkringer, *Dalton Trans.*, 2020, **49**, 274–278.
21 H. Ohno, *Electrochem. Aspects Ionic Liq.*, 2005, 1–392.
22 K. Binnemans, *Chem. Rev.*, 2007, **107**, 2592–2614.
23 T. Welton, *Chem. Rev.*, 1999, **99**, 2071–2083.
24 A. V. Mudring and S. Tang, *Eur. J. Inorg. Chem.*, 2010, 2569–2581.
25 Z. Lei, B. Chen, Y. M. Koo and D. R. Macfarlane, *Chem. Rev.*, 2017, **117**, 6633–6635.
26 J. Dupont, G. S. Fonseca, A. P. Umpierre, P. F. P. Fichtner and S. R. Teixeira, *J. Am. Chem. Soc.*, 2002, **124**, 4228–4229.
27 D. S. Jacob, L. Bitton, J. Grinblat, I. Felner, Y. Koltypin and A. Gedanken, *Chem. Mater.*, 2006, **18**, 3162–3168.
28 C. Zhang, J. Chen, Y. Zhou and D. Li, *J. Phys. Chem. C*, 2008, **112**, 10083–10088.
29 D. W. Davidson and S. K. Garg, *Can. J. Chem.*, 1972, **50**, 3515–3520.
30 P. Goyal, A. Sengupta, A. Srivastava, S. Mukherjee, V. V. Rout and P. K. Mohapatra, *Inorg. Chem.*, 2024, **63**, 7161–7176.
31 H. Jang, Development of Uranium Fluoride Microstructures (2024), UNLV Theses, Dissertations, *Professional Papers, and Capstones*, 5179, DOI: 10.34917/38330391.
32 C. Xu and Z. Cheng, *Processes*, 2021, **9**, 337.
33 C. Maton, N. De Vos and C. V. Stevens, *Chem. Soc. Rev.*, 2013, **42**, 5963–5977.
34 R. E. Del Sesto, T. M. McCleskey, C. Macomber, K. C. Ott, A. T. Koppisch, G. A. Baker and A. K. Burrell, *Thermochim. Acta*, 2009, **491**, 118–120.
35 M. J. Earle, C. M. Gordon, N. V. Plechkova, K. R. Seddon and T. Welton, *Anal. Chem.*, 2007, **79**, 758–764.
36 A. C. Momin, E. B. Mirza and M. D. Mathews, *J. Nucl. Mater.*, 1991, **185**, 308–310.
37 S. Kern, J. Hayward, S. Roberts, J. W. Richardson, F. J. Rotella, L. Soderholm, B. Cort, M. Tinkle, M. West, D. Hoisington and G. H. Lander, *J. Chem. Phys.*, 1994, **101**, 9333–9337.
38 J. Ranke, A. Othman, P. Fan and A. Müller, *Int. J. Mol. Sci.*, 2009, **10**, 1271.
39 J. G. McDaniel and A. Verma, *J. Phys. Chem. B*, 2019, **123**, 5343–5356.
40 R. D. Rogers, D. Macfarlane, S. Zhang, Y. Kohno and H. Ohno, *Chem. Commun.*, 2012, **48**, 7119–7130.
41 R. F. Rodrigues, A. A. Freitas, J. N. Canongia Lopes and K. Shimizu, *Molecules*, 2021, **26**, 7159.
42 L. Cammarata, S. G. Kazarian, P. A. Salter and T. Welton, *Phys. Chem. Chem. Phys.*, 2001, **3**, 5192–5200.
43 V. H. Paschoal, L. F. O. Faria and M. C. C. Ribeiro, *Chem. Rev.*, 2017, **117**, 7053–7112.
44 H. Jang and F. Poineau, *ACS Omega*, 2024, **9**, 26380–26387.